Optik 126 (2015) 1156–1160

Contents lists available at ScienceDirect

Optik

journal homepage: www.elsevier.de/ijleo

Room temperature performance analysis of bilayer graphene terahertz photodetector

M. Mohammadian, H. Rasooli Saghai*

Department of Electrical Engineering, Tabriz Branch, Islamic Azad University, Tabriz, Iran

ARTICLE INFO

Article history:
Received 19 February 2014
Accepted 4 March 2015

Keywords:
Bilayer graphene terahertz photdetector
Dark current
Detectivity
Room temperature
Responsivity

ABSTRACT

In this paper, the room temperature performance of bilayer graphene terahertz photodetector is studied by calculating of its dark current and dark current limited detectivity at room temperature. In the first step the spectral dependences of the photodetector responsivity as function of the device structural parameters is calculated. It is demonstrated that at the radiation frequency close to the resonant frequencies of plasma oscillations, the responsivity can exhibit sharp and very high maxima corresponding to fairly large responsivity values. In the second step the dark current and dark current limited detectivity for different temperatures, bias voltage, and widths of graphene layer is calculated and analyzed. The obtained results show that for the bilayer graphene photodetector with $W = 5$ nm, $L = 20$ μm, $V_b = 2$ V, $V_g = 2$ V, value of dark current limited detectivity D^*, at room temperature $T = 300$ °K and also $T = 200$ °K are 9×10^6 $\left(\text{cm}\sqrt{\text{Hz}}/\text{W}\right)$ and $\sim 6 \times 10^9$ $\left(\text{cm}\sqrt{\text{Hz}}/\text{W}\right)$, respectively.

1. Introduction

Carbon is the material prima for life on the planet and the basis of all organic chemistry. Because of the flexibility of its bonding, carbon based systems show an unlimited number of different structures with an equally large variety of physical properties. These physical properties are, in great part, the result of the dimensionality of these structures. Among systems with only carbon atoms, graphene – a two dimensional (2D) allotrope of carbon – plays an important role since it is basis for the understanding of the electronic properties in other allotropes. Graphene is made up of carbon atoms arranged on a honeycomb structure made up of hexagons. Graphene provides a lot of more interesting physics in addition to being a purely two dimensional crystal of only one atomic layer thickness. Graphene has a unique electronic structure, which is fundamentally different from anything that was known before. Due to its linear dispersion relation at low energies, the electrons are turned into effective Dirac fermions. In most IR photodetectors and imaging devices, the narrow gap semiconductor structures such as HgCdTe and InSb have been utilized [1,2]. The necessity of further extension of the wavelength range covered by photodetectors, widening of functionality, as well as cost reduction in production processes has stimulated the development of low dimensional structure like quantum well, quantum dot, and quantum wire infrared (IR) photodetectors [3,4]. On the other hand, there has been a great deal of recent interest in the optoelectronic device based on planar carbon structures, which have unique electronic and optical properties [5,6]. In comparison of bilayer based IR photodetector with traditional photodetectors based on narrow gap and gapless bulk material like HgCdTe [7,8], the main advantage of this detectors is operating at the higher temperature because of their lower thermo-generation rate. Also in contrast with material like HgCdTe in which the Auger generation–recombination processes play an important role [9], such processes in graphene layers are forbidden [10].

In this paper, we model the bilayer graphene IR-photodetector and calculate the photodetector parameters such as dark current and dark current limited detectivity, D^*, as a function of the gate voltage, graphrn layer (GL) width and temperature, especially at room temperature.

2. Structure of bilayer graphene photodetector and its responsivity

We consider the IR photodetector which is shown in Fig. 1(a) and (b), where the detection area consists of two graphene layers separated by a thin barrier layer hBN [11]. Each GL is supplied by an ohmic side contact (left – side contact to lower GL and right – contact to upper GL). It is assumed that a dc bias voltage is V_0

* Corresponding author. Tel.: +98 411 3328560; fax: +98 411 3328560.
E-mail address: h_rasooli@iaut.ac.ir (H.R. Saghai).

http://dx.doi.org/10.1016/j.ijleo.2015.03.021
0030-4026/

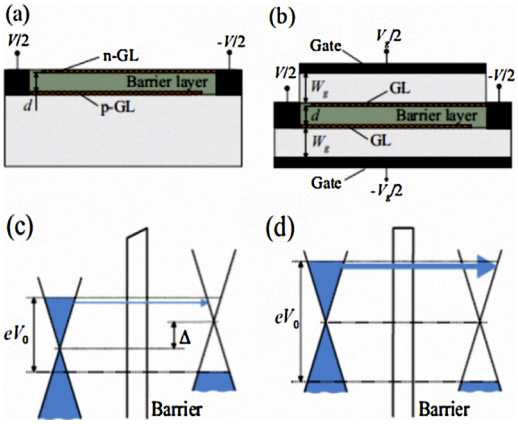

Fig. 1. Schematic views of (a) a doped double – GL structure and (b) a gated double-GL structure with electrical doping, and (c), (d) band diagram.

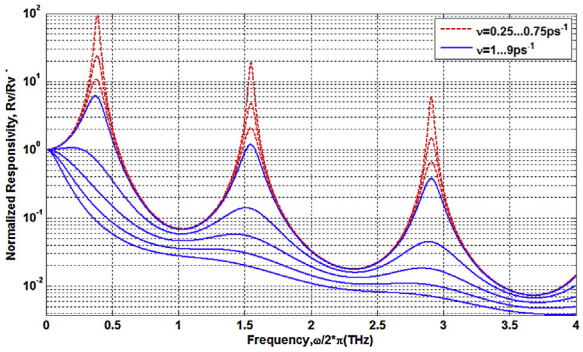

Fig. 2. Normalized detector responsivity as a function of radiation frequency $\omega/2\pi$ for double – GL heterostructures with different collision frequencies of electron and holes υ: dashed lines, $\upsilon = (0.25–0.75)\ \mathrm{ps}^{-1}$ and solid lines, $\upsilon = (1–9)\ \mathrm{ps}^{-1}$.

applied between these contacts. Due to this, electron (in the upper GL) and hole (in the lower GL) formed as shown schematically in Fig. 1(c). In Fig. 1(a) double GL structure chemically doped GL and Fig. 1(b) undoped GLs. In the first case, one of the GLs is doped by donors, whereas the other one is doped by acceptors, so that the electron and hole sheet densities in the pertinent GLs are equal to the dopant density (donors and acceptors). In the second case the voltage gate applied between the gates, induces the electrons and holes. The incoming THz signal transforms into the ac voltage $\delta V \pm = \pm\frac{\delta V(t)}{2} = \pm\left(\frac{\delta V}{2}\right)\exp(-i\omega t)$ at the contacts, where ω is the THz signal frequency.

The variation of the terminal current (between GLs), δJ, associated with the incoming THz signal, includes the displacement and tunneling components [12]:

$$\delta J = -i\omega C\delta V + H\int_{-1}^{1} \mathrm{d}x\, j_t \tag{1}$$

where the tunneling current density is given by:

$$\delta j_t = \sigma_t\left(\delta\varphi_+ - \delta\varphi_-\right) + \beta_t(\delta\varphi_+ - \delta\varphi_-) \tag{2}$$

where C is the double-GL heterostructure capacitance including the geometrical and quantum capacitances [12,13].

The gate voltage V_g, changes the Fermi energy level and induces carriers to the detection area with the length L ($V_g > 0$ induce electron and $V_g < 0$ induce hole to the graphene layers). The incident IR radiation with $\hbar\omega > E_g$ can excite carriers to the conduction band. Within the conduction band the carriers can be swept by low bias voltage V_b. By increasing the gate voltage, the Fermi level which located at $E_f = 0$ for $V_g = 0$, moves higher energies until reaches to the minimum energy of the conduction (valance) band, which we call this point threshold voltage V_t. For $|V_g| > V_t$, carriers induce to the detection region. That value of V_t depends on the band structure and the energy gap of GL. The rectified component, δJ_0, of the variation of the terminal current, δJ, given by [14]:

$$J_0 = \frac{\beta(\delta V)^2 LH}{\left|\cos\gamma L - \gamma L\sin\gamma L\right|^2}\int_{-1}^{1}\mathrm{d}\xi\left|\cos\left(\gamma L\xi\right)\right|^2 \tag{3}$$

Considering that $(\delta V)^2$ is proportional to the power of the THz radiation received by the antenna, P_w, introducing the characteristic responsivity of the tunneling detector under consideration $\bar{R}\upsilon$ (which corresponds to the situation when the plasma affects are insignificant, so that each GL is equipotential). The normalized responsivity given by [15]:

$$\begin{aligned}\frac{R\upsilon}{\bar{R}\upsilon} &= \frac{1}{2}\int_{-1}^{1}\mathrm{d}\xi\left\{\cos^2\left[\left(\frac{\pi\sqrt{\omega\sqrt{\omega^2+\upsilon^2}}}{\Omega}\cos\Theta\right)\xi\right] + \sinh^2\left[\left(\frac{\pi\sqrt{\omega\sqrt{\omega^2+\upsilon^2}}}{\Omega}\sin\Theta\right)\xi\right]\right\}\\ &\times\left|\cos\left(\frac{\pi\sqrt{\omega\sqrt{\omega^2+\upsilon^2}}}{\Omega}e^{i\Theta}\right) - \left(\frac{\pi\sqrt{\omega\sqrt{\omega^2+\upsilon^2}}}{4\Omega\Omega}e^{i\Theta}\right)\times\sin\left(\frac{\pi\sqrt{\omega\sqrt{\omega^2+\upsilon^2}}}{\Omega}e^{i\Theta}\right)^{-2}\right|\\ &= \frac{1}{2}\left[\frac{\sin\left(\left(2\pi\sqrt{\omega\sqrt{\omega^2+\upsilon^2}}/\Omega\right)\cos\Theta\right)}{\left(\left(2\pi\sqrt{\omega\sqrt{\omega^2+\upsilon^2}}/\Omega\right)\cos\Theta\right)} + \frac{\sin h\left(\left(2\pi\sqrt{\omega\sqrt{\omega^2+\upsilon^2}}/\Omega\right)\sin\Theta\right)}{\left(\left(2\pi\sqrt{\omega\sqrt{\omega^2+\upsilon^2}}/\Omega\right)\sin\Theta\right)}\right]\\ &\times\left|\cos\left(\frac{\pi\sqrt{\omega\sqrt{\omega^2+\upsilon^2}}}{\Omega}e^{i\Theta}\right) - \left(\frac{\pi\sqrt{\omega\sqrt{\omega^2+\upsilon^2}}}{\Omega}e^{i\Theta}\right)\times\sin\left(\frac{\pi\sqrt{\omega\sqrt{\omega^2+\upsilon^2}}}{\Omega}e^{i\Theta}\right)^{-2}\right|\end{aligned} \tag{4}$$

That υ is collision frequency of electrons and holes in GLs with impurities and acoustic phonons, and $\theta = \frac{1}{2}\tanh^{-1}(\upsilon/\omega)$. The results of numerical calculation using Eq. (4) are shown in Figs. 2–4.